

Flexural response of piles under liquefied soil conditions

R. S. Meera · K. Shanker · P. K. Basudhar

Received: 23 April 2006 / Accepted: 1 November 2006 / Published online: 6 December 2006
© Springer Science+Business Media B.V. 2006

Abstract The paper pertains to the development of a generalized procedure to analyze and predict the flexural behavior of axially and laterally loaded pile foundations under liquefied soil conditions. Pseudo-static analysis has been carried out taking into consideration the combined effect of axial load and lateral load. Based on the available literature effect of degradation on the modulus of subgrade reaction due to soil liquefaction has been incorporated in the analysis. The developed program was calibrated and validated by comparing the predicted behavior of the pile with theoretical and experimental results reported in literature. The predicted behavior has been found to be in excellent to very good agreement with the theoretical and observed values in the field, respectively. The present study highlights the importance of considering the axial load from the superstructure along with the inertia forces from the superstructure and the kinematic forces from the liquefied soil in the design of pile foundations in liquefiable areas. The significance of densification of the soil in the

liquefiable areas and presence of an adequate top non-liquefied soil cover causing appreciable reduction in deflection and bending moment experienced by the piles has been highlighted.

Keywords Axially and laterally loaded piles · Flexural behavior · Lateral spreading · Liquefaction · Pseudo-static analysis · Soil-structure interaction · Subgrade reaction

Notations

a, b, c, d, e, f, g, h	Coefficients of boundary conditions;
A	Stiffness matrix
B	Force vector
C	Modified displacement coefficient matrix
D	Diameter of the pile
E_p	Modulus of elasticity of the pile
E_s	Modulus of elasticity of the soil
E_0	Modulus of deformation of the soil
F	Displacement coefficient matrix
$\{g\}$	Ground displacement vector
g_{\max}	Maximum possible permanent horizontal ground displacement of the liquefied soil

R. S. Meera · K. Shanker · P. K. Basudhar (✉)
Civil Engineering Department, Indian Institute of
Technology Kanpur, Kanpur 208016, India
e-mail: pkbd@iitk.ac.in

K. Shanker
e-mail: kandukurishanker@yahoo.com

g_{rs}	Permanent horizontal displacement of the level ground far away from the water front	N N_a	Standard penetration test value Axial load distribution matrix
g_w	Displacement of the quay wall	\mathbf{O}	Applied force vector
g_x	Horizontal ground displacement at a distance x from the waterfront	p P	Soil pressure Axial load applied at the pile top
$g(z, x)$	Permanent horizontal ground displacement profile with depth, z at a distance, x from the waterfront	P_z Q	Axial load variation with depth z Soil modulus to soil strength ratio
g_0	Permanent horizontal ground displacement at the waterfront	r R s	Non-liquefied depth factor Pile flexibility factor Liquefied depth factor
G	Modification factor	sl	Gradient of the surface topography
H	Horizontal load factor		
H_T	Horizontal load applied at the pile top	S_f	Stiffness degradation parameter
I_p	Moment of inertia of the pile	S_u	Un-drained strength of the soil
\mathbf{J}	Coefficient matrix		
\mathbf{k}	Matrix for the modulus of subgrade reaction	t T	Embedded depth factor Lateral soil force vector
k_h	Modulus of subgrade reaction	U	Matrix for the equilibrium conditions
k_{hn}	Modulus of subgrade reaction for non-liquefied soils	V	Vertical load factor
K	Stiffness factor	x	Distance of the location of the pile from the waterfront
L	Length of the pile		
L_s	Affected distance of lateral spreading	y y_r	Deflection of the pile Relative displacement of the pile and the soil
L_x	Location factor		
L_1	Thickness of the top non-liquefiable soil cover	y_1 Y	Reference value for y_r Non-dimensional deflection coefficient
L_2	Thickness of the liquefiable layer	Y^*	Maximum non-dimensional deflection coefficient
L_3	Length of pile embedded into the bottom non-liquefiable layer	z Z	Depth Non-dimensional depth coefficient
L/D	Length to diameter ratio		
M	Moment factor	β	Axial load variation coefficient
M_D	Developed bending moment		
M_T	Moment applied at the pile top		
M'	Non-dimensional bending moment coefficient		
M^*	Maximum non-dimensional bending moment coefficient		
$n + 1$	Number of elements		

1 Introduction

Importance of liquefaction related damage to the piles has been amply revealed during past

earthquakes, from the 1964 Niigata earthquake to the 1995 Kobe earthquake. Permanent ground displacement induced by soil liquefaction is among the serious liquefaction hazards. Many civil engineering structures, especially lifeline facilities are mostly affected by the liquefaction induced permanent ground displacement.

The offshore piles are subjected to combined loading and they are more prone to the attack of liquefaction-induced lateral spreading. The analysis of the load–displacement behavior of a pile is a complex soil–structure interaction problem. Lack of availability of correct information regarding the actual failure and deformation patterns of piles in liquefiable areas magnifies the complexity of the phenomenon. As such, analysis and design procedures for piles in liquefying grounds have large uncertainties due to a lack of physical data and proper understanding of the physical mechanisms involved. However, the analysis is simplified by assuming the pile to be responding pseudo-statically to the lateral permanent displacement of the ground. A brief overview of the subject is presented as follows.

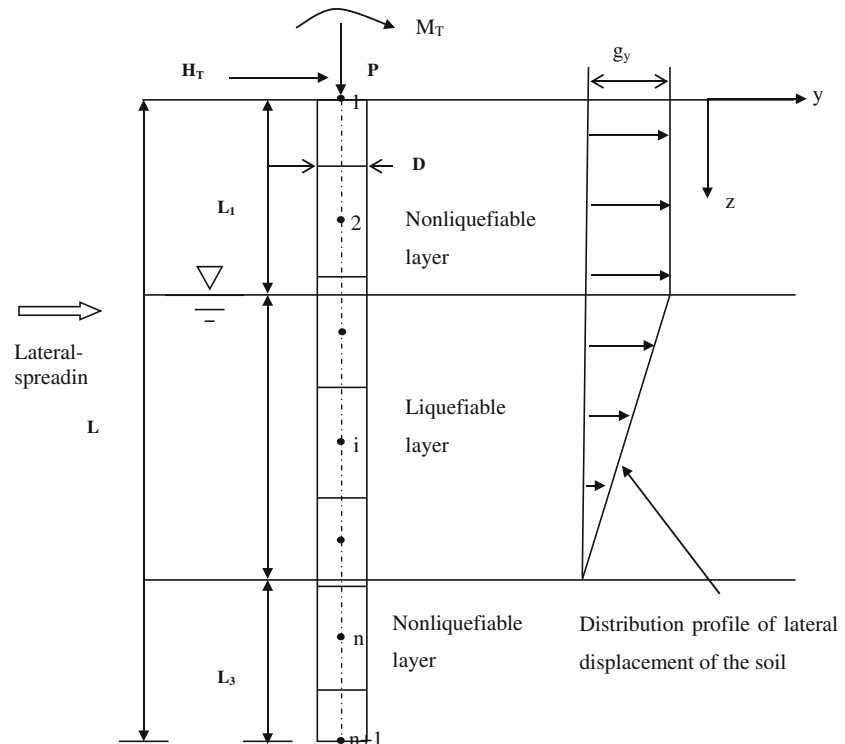
Hamada and O'Rourke (1992) investigated liquefaction induced permanent ground deformation and lifeline performance during past earthquakes in Japan and USA from the 1906 San Francisco earthquake to the 1989 Loma Prieta earthquake through the Japan–US cooperative research program. Thereafter many studies have been performed (Mishra 1992; Miyajima and Kitaura 1994; O'Rourke et al. 1994; Barlett and Youd 1995; Ishihara and Cubrinovski 1998; Tokimatsu et al., 1998; Berril et al. 2001; Abdoun and Dobry 2002; Tamari and Towhata 2003; Bhattacharya 2004; Klar et al. 2004; Zhang et al. 2004) leading to better understanding of the problem. These papers clarify the mechanisms of generation of liquefied ground flow, estimation of the value of permanent ground displacement and the flexural behavior. Experimental studies made it possible to develop empirical correlations for estimating the permanent ground movement; pressure exerted by the laterally spreading soil and degraded subgrade modulus arising out of softening of soils due to liquefaction. The effect of lateral spreading force on the flexural behavior of piles and the analysis of laterally loaded piles

under liquefied soil conditions have also been studied and relationships are available in the form of non-dimensional charts (Basudhar et al. 2002). Significant effect of loss of support on the buckling of slender piles has also drawn the attention of researchers and a few works have been reported (Bhattacharya 2004). But very few studies have been conducted to find the response of piles under combined loadings and liquefied soil conditions.

In view of the above review, an attempt is made here to analyze the flexural behavior of axially and laterally loaded piles under liquefied soil conditions. The external loads such as the axial load from the superstructure and the lateral loads due to the inertial effects, wind, waves, etc., are considered along with the kinematic effects of permanent ground displacement. The relative displacement of soil and pile and the degradation in the stiffness of soil due to liquefaction have been considered in the present analysis assuming the validity of the Winkler's idealization of the soil being made up of discrete springs.

2 Statement of the problem

The idealization of the pile and the soil profile surrounding the pile for the assessment of the soil–pile interaction is shown in Fig. 1. A pile of length, L and diameter, D is embedded in a homogeneous saturated sand deposit. The water table is at the top of a liquefiable stratum of thickness, L_2 , above which is the non-liquefiable soil cover of thickness, L_1 . Below the liquefiable stratum there is a firm, non-liquefiable soil layer. The pile is further embedded by a distance L_3 into this non-liquefiable stratum. Over the depth L_2 , the soil is in a liquefied state and the pile has lost the support of the soil either completely or partially. The pile is subjected to a lateral load, H_T and a moment, M_T along with an axial load, P at the top. In this problem, the possible movement of the liquefied soil in the liquefied zone has also been considered. The liquefied soil flows with a maximum velocity at the ground level and the maximum soil displacement, g_x is at the ground surface and it varies with depth and its' value being zero at the lower end of the liquefied zone.

Fig. 1 Definition sketch

This flowing mass will cause a drag force on the pile. There are various possible distributions of soil displacement. A trapezoidal distribution is applied in the figure.

Thus for given inputs of L_1 , L_2 , L_3 and soil and pile properties, the objective is to find the flexural behavior of the pile when it has lost the supporting capacity of the soil to a great extent over the specified length of the pile due to soil liquefaction. The effect of different types of loading, end conditions and the various soil parameters on the deflection as well as bending moment distribution of the pile along the length has to be determined.

3 Analysis

3.1 Modulus of sub-grade reaction

A simplified pseudo-static design method using the concept of modulus of sub-grade reaction theory based on Winkler soil model has been adopted in this study. In this approach the soil pressure, p and the lateral deflection, y at a point

are assumed to be related through a modulus of subgrade reaction, k_h . Thus,

$$p = k_h y \quad (1)$$

where k_h has the units of force/length³.

For cohesionless soils the value of k_h is not constant and generally varies with depth; in case of homogeneous cohesionless soil deposits k_h generally increases linearly with depth. In order to take care of the arbitrary variation of the k_h in the soil deposits it is convenient to correlate it with the SPT, N values. The modulus of subgrade reaction for non-liquefied soils, k_{hn} as proposed by Architecture Institute of Japan 2001 and Japan Road Association 1997 has been adopted here as follows,

$$k_{hn} = 80E_0D^{(-0.75)} \quad (2)$$

$$E_0 = 0.7N \quad (3)$$

in which E_0 is the modulus of deformation in MN/m², N is the SPT-value, and D is the diameter of the pile in centimeters.

As soil liquefies, the stiffness of soil degrades and from case studies it has been found that the modulus of subgrade reaction for the laterally spreading soils are reduced by a scaling factor termed as Stiffness degradation parameter, S_f varies from 0.001 to 0.01 (Ishihara 1997). The degradation of k_{hn} with increasing displacement is expressed as (Tokimatsu 1999)

$$k_h = (k_{hn}) \frac{1}{1 + |y_r/y_1|} \tag{4}$$

where y_r is the relative displacement between ground and pile and y_1 is the reference value of y_r .

In reality, Eq. (1) may not be effective where the ground displacements are large. Hence the soil is assumed to be a Winkler-type material with lateral soil force proportional to the relative displacement between pile and soil. Thus the modified equation is

$$p = k_h(y - g(z, x)) \tag{5}$$

where, $g(z, x)$ is the permanent ground displacement profile with depth, z , near the pile.

When lateral spreading occurs near the waterfront, the permanent horizontal ground displacement generally decreases towards inland with a maximum value at the waterfront. The affected distance of such lateral spreading from the waterfront, L_s is given as (Tokimatsu 1999),

$$L_s/L_2 = (25-100)g_0/L_2 \tag{6}$$

where, g_0 is the permanent horizontal ground displacement at the waterfront and is defined as,

$$g_0 = \min(g_{max}, g_w) \tag{7}$$

in which g_w is the displacement of the quay wall and g_{max} is the maximum possible permanent ground surface displacement of the liquefied soil. g_{max} is found out using the following relation (Hamada et al. 1986),

$$g_{max} = 0.75(L_2)^{0.5}(sl)^{0.33} \tag{8}$$

where, g_{max} and L_2 are in meters and sl is the slope of the base of the liquefied layer or the

gradient of the surface topography whichever is maximum.

The horizontal ground displacement at a distance; x from the waterfront, g_x is expressed in a normalized form and defined as (Shamoto et al. 1998),

$$g_x/g_0 = (0.5)^{(5x/L_s)} + \{1 - (0.5)^{(5x/L_s)}\}g_{rs}/g_0 \tag{9}$$

where g_{rs} is the permanent horizontal displacement of the level ground far away from the waterfront and may be assumed to be zero.

Following Tokimatsu (1999), the permanent horizontal ground displacement profile with depth, z at a distance, x of a laterally spreading deposit, $g(z, x)$ is approximated as,

$$\begin{aligned} \text{For } z < L_1, g(z, x) &= g_x \\ \text{For } z > L_1 \text{ and } z < (L_1 + L_2), g(z, x) &= g_x \left[\cos \left\{ \frac{\pi(z - L_1)}{2L_2} \right\} \right] \\ \text{For } z > (L_1 + L_2), g(z, x) &= 0 \end{aligned} \tag{10}$$

3.2 Governing differential equation

For an elastic pile of constant stiffness $E_p I_p$ and diameter D embedded in a Winkler medium and subjected to an axial load, P at the pile head, the governing differential equation for the horizontal deflection, y along the pile is (Hetenyi 1946)

$$E_p I_p \frac{d^4 y}{dz^4} + \frac{d}{dz} \left[P_z \frac{dy}{dz} \right] = -pD \tag{11}$$

in which E_p and I_p are Young’s modulus and moment of inertia of pile, respectively. Substituting Eq. (5) in Eq. (11), we get

$$E_p I_p \frac{d^4 y}{dz^4} + \frac{d}{dz} \left[P_z \frac{dy}{dz} \right] + k_h D (y - g(z, x)) = 0. \tag{12}$$

Solutions to the above equation can be conveniently obtained by using finite difference method. Referring to Fig. 1, the pile is divided into $(n + 1)$ elements of which $(n-1)$ elements are of

equal length and the other two, one at the top and the other at the bottom, are of half the length of these elements. The nodes of the elements are considered at their centers with one node at the head of the pile and the other at its tip. The soil is assumed to be an ideal, homogeneous, isotropic, and an elastic half space, having Young’s modulus, E_s , which is unaffected by the presence of the pile. The axial load distribution depends on E_s and hence this parameter is considered.

3.3 Solution technique and boundary conditions

Using central difference technique, the governing differential equation can be expressed in finite difference form in terms of the nodal deflections. For a typical node i on the pile, Eq. (12) can be written as

$$\begin{aligned} & \frac{E_p I_p n^4}{L^4} [y_{i-2} - 4y_{i-1} + 6y_i - 4y_{i+1} + y_{i+2}] + \\ & \frac{Pn^2}{L^2} \left[\left\{ \alpha_i - \frac{(\alpha_{i+1} - \alpha_{i-1})}{4} \right\} y_{i-1} - 2\alpha_i y_i \right. \\ & \left. + \left\{ \alpha_i + \frac{(\alpha_{i+1} - \alpha_{i-1})}{4} \right\} y_{i+1} \right] \\ & + k_h D(y - g) = 0 \end{aligned} \tag{13}$$

where $\alpha_i = P_i/P$ and P_i is the axial load acting at node i .

For nodes 2 and n , the equation consists of the displacements at the imaginary nodes considered at the top (node 0) and tip of the pile (node $(n + 2)$). These imaginary displacements are to be evaluated by employing the relevant boundary conditions.

The axial load variation is assumed to be linear in the present analysis which can be expressed in the form

$$P(z) = P(1 - \beta(z/L)) \tag{14}$$

where $P(z)$ is the axial load at any depth z . P is the axial load at the pile head, L is the length of the pile and β is the variation coefficient.

We need to have two more equations that are obtained from the force and the moment equilibrium equations.

Table 1 Bombay condition

End conditions	Relevant boundary values
Free–Free	$E_p I_p y'' = M_T$, at $z = 0$ $E_p I_p y'' = 0$, at $z = L$
Fixed–Free	$E_p I_p y' = 0$, at $z = 0$ $E_p I_p y'' = 0$, at $z = L$
Fixed–Free	$E_p I_p y' = 0$ & $E_p I_p y = 0$, at $z = 0$ $E_p I_p y'' = 0$, at $z = L$
Fixed–Pinned	$E_p I_p y' = 0$ & $E_p I_p y = 0$, at $z = 0$ $E_p I_p y'' = 0$ & $E_p I_p y = 0$, at $z = L$
Fixed–Fixed	$E_p I_p y' = 0$ & $E_p I_p y = 0$, at $z = 0$ $E_p I_p y' = 0$ & $E_p I_p y = 0$, at $z = L$

$$\begin{aligned} & \sum M_{(\text{about pile tip})} \\ & = 0(0.5n00.125 \ n - 1 \ n - 2 \\ & \dots \dots \dots \ n - i + 1 \ .. \ 1 \ 0.125) \end{aligned} \tag{15}$$

$$\{p_i D\} = \frac{H_T n^2}{L} + \frac{M_T n^2}{L^2}$$

$$\begin{aligned} & \sum H = 0 \\ & (0.5 \ 1 \ 1 \ \dots \ \dots \ \dots \ 1 \ \dots \ 1 \ 0.5) \{p_i D\} = \frac{H_T n}{L} \end{aligned} \tag{16}$$

The various boundary conditions considered in the present analysis are presented in Table 1. The end conditions are: Free–Free, Fixed–Free, Fixed–Pinned and Fixed–Fixed. Thus having $(n + 1)$ equations in $(n + 1)$ unknowns, the simultaneous equations can be solved using Gauss elimination technique. The equations are written in non-dimensional form and expressed in the matrix form as follows.

$$\mathbf{A}\mathbf{Y} = \mathbf{B} \tag{17}$$

in which \mathbf{A} is the stiffness matrix of size $(n + 1)$, \mathbf{Y} is the displacement column vector of size $(n + 1)$ and \mathbf{B} is the force column vector of size $(n + 1)$.

The stiffness matrix, \mathbf{A} , is obtained by

$$\mathbf{A} = \mathbf{C} + \mathbf{J} \tag{18}$$

where \mathbf{C} is the modified displacement coefficient matrix of size $(n + 1)$ and \mathbf{J} is a coefficient matrix of size $(n + 1)$. \mathbf{C} is defined as,

$$\mathbf{C} = \mathbf{F} + \mathbf{G}\mathbf{N}_a \tag{19}$$

in which \mathbf{F} is the displacement coefficient matrix of size $(n + 1)$.

$$\mathbf{F} = \begin{bmatrix} 0 & 0 & 0 & 0 & 0 & 0 & 0 & 0 & 0 & 0 \\ a & b & c & d & 0 & 0 & 0 & 0 & 0 & 0 \\ 1 & -4 & 6 & -4 & 1 & 0 & 0 & 0 & 0 & 0 \\ 0 & 1 & -4 & 6 & -4 & 1 & 0 & 0 & 0 & 0 \\ \cdot & \cdot & \cdot & \cdot & \cdot & \cdot & \cdot & \cdot & \cdot & \cdot \\ \cdot & \cdot & \cdot & \cdot & \cdot & \cdot & \cdot & \cdot & \cdot & \cdot \\ 0 & 0 & 0 & 0 & 1 & -4 & 6 & -4 & 1 & 0 \\ 0 & 0 & 0 & 0 & 0 & 1 & -4 & 6 & -4 & 1 \\ 0 & 0 & 0 & 0 & 0 & 0 & e & f & g & h \\ 0 & 0 & 0 & 0 & 0 & 0 & 0 & 0 & 0 & 0 \end{bmatrix} \tag{20}$$

a, b, c, d, e, f, g, h are elements which depends on the boundary conditions and they are given in Table 2.

G is the modification factor expressed as

$$G = \frac{\pi}{4Rn^2 \left(\frac{L}{D}\right)^2} \cdot \frac{P}{\pi D^2 E_s} \tag{21}$$

where $R = E_p I_p / E_s L^4$ is the pile flexibility factor and E_s is the modulus of elasticity of soil.

\mathbf{N}_a the axial load distribution matrix of size $(n + 1)$ is defined as, for $i = 2$ to n ,

$$\begin{aligned} \mathbf{N}_a(i, i - 1) &= \left[\left\{ \alpha_i - \frac{(\alpha_{i+1} - \alpha_{i-1})}{4} \right\} \right], \mathbf{N}_a(i, i) = -2\alpha_i \\ \mathbf{N}_a(i, i + 1) &= \left[\left\{ \alpha_i + \frac{(\alpha_{i+1} - \alpha_{i-1})}{4} \right\} \right], \\ \mathbf{N}_a(1, i) &= \alpha_i^t - \alpha_i^b \\ \mathbf{N}_a(1, 1) &= -\alpha_1^b, \mathbf{N}_a(1, n + 1) = \alpha_{n+1}^t \\ \mathbf{N}_a(n + 1, i) &= 0 \text{ for } i = 1 \text{ to } n + 1, \end{aligned} \tag{22}$$

where $\alpha_i, \alpha_i^t, \alpha_i^b$ are the P_i/P values at the centre, top and tip of a pile element, respectively.

The coefficient matrix of size $(n + 1)$, \mathbf{J} accounts for the matrix for the horizontal load

Table 2 Boundary condition coefficients

End conditions	Elements of the <i>F</i> matrix							
	<i>a</i>	<i>b</i>	<i>c</i>	<i>d</i>	<i>e</i>	<i>f</i>	<i>g</i>	<i>H</i>
Free-Free	-2	5	-4	1	1	-4	5	-2
Fixed-Free (no sway)	0	7	-4	1	1	-4	5	-2
Fixed-Free (with sway)	-4	7	-4	1	1	-4	5	-2
Fixed-Pinned	0	7	-4	1	1	-4	5	0
Fixed-Fixed	0	7	-4	1	1	-4	7	0

and moment equilibrium conditions, U and the matrix for the modulus of subgrade reaction, k .

\mathbf{J} is expressed as

$$\mathbf{J} = \left(\frac{[U]}{Rn^4} \right) * \frac{D[k]}{E_s} \tag{23}$$

where

$$U = \begin{bmatrix} 0.5n-0.125 & n-1 & n-2 & \dots & n-i+1 & \dots & 1 & 0.125 \\ 0 & 1 & 0 & 0 & 0 & 0 & 0 & 0 & 0 \\ - & - & - & - & - & - & - & - & - \\ 0 & 0 & 0 & 0 & 0 & 0 & 0 & 0 & 0 \\ 0.5 & 1 & 1 & 1 & 1 & 1 & 1 & 1 & 0.5 \end{bmatrix} \tag{24}$$

The matrix for modulus of subgrade reaction k is a diagonal matrix of size $(n + 1)$ and is defined as

$$\text{for } i = 1 \text{ to } n + 1, \mathbf{k}(i, i) = k_h \text{ at node } i. \tag{25}$$

The displacement column vector, Y is defined as

$$\text{for } i = 1 \text{ to } n + 1, \mathbf{Y}(i) = y_i/D \tag{26}$$

The force vector \mathbf{B} can be found out using the relation

$$\mathbf{B} = \mathbf{O} + \mathbf{T} \tag{27}$$

where \mathbf{O} is the applied force vector.

For Free-Free end condition,

$$\mathbf{O} = \left(\frac{1}{Rn^2 \left(\frac{L}{D}\right) \left(\frac{E_s}{S_u}\right)} \right) * \left\{ \begin{array}{c} \frac{H_T}{S_u D^2} + \frac{M_T}{S_u D^3 \frac{L}{D}} \\ \frac{-M_T}{S_u D^3 \frac{L}{D}} \\ 0 \\ - \\ 0 \\ \frac{H_T}{S_u D^2 n} \end{array} \right\} \tag{28}$$

For other end conditions,

$$\mathbf{O} = \left(\frac{1}{Rn^2 \left(\frac{L}{D}\right) \left(\frac{E_s}{S_u}\right)} \right) * \left\{ \begin{array}{c} \frac{H_T}{S_u D^2} + \frac{M_T}{S_u D^3 \frac{L}{D}} \\ 0 \\ 0 \\ - \\ 0 \\ \frac{H_T}{S_u D^2 n} \end{array} \right\} \tag{29}$$

in which S_u is the undrained strength of the soil.

\mathbf{T} , the lateral soil force vector is,

$$\mathbf{T} = [J] \times \frac{\{g\}}{D} \tag{30}$$

where g is the ground displacement vector obtained from the permanent horizontal ground displacement profile.

The developed bending moment is M_D . The non-dimensional bending moment coefficient, M' can be found out using

$$M' = \frac{M_D}{S_u D^3} = \frac{E_p I_p}{S_u D^3} \left(\frac{d^2 y}{dz^2} \right) \tag{31}$$

Using Matlab, computer programs have been developed for the analysis.

4 Calibration of the program

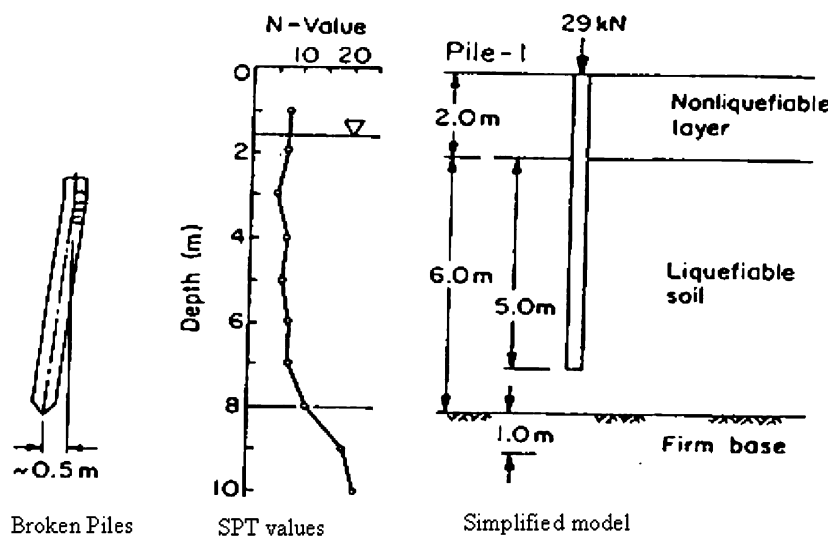
The developed program is calibrated in the following way. Results were obtained for a Free–Free pile and Fixed–Free pile subjected to horizontal load and embedded in a homogeneous non-liquefied soil layer in which k_h is constant with depth. The parameters chosen for Free–Free pile are $Z = 1$, $H = 25$, $L/D = 25$, $k_h D/E_s = 0.3$, $Q = 200$ and $R = 0.1$. The parameters chosen for Fixed–Free pile are $Z = 1$, $H = 25$, $L/D = 25$, k_h

$D/E_s = 0.3$, $Q = 100$ and $R = 0.01$. The results (computed by using 20 elements) were then compared with the closed form solution developed by Hetenyi (1946). The deflection coefficient at the ground line for the Free–Free pile is obtained as 0.067 and the corresponding solution for the horizontal displacement given by Hetenyi provided identical result. For the Fixed–Free pile the predicted deflection coefficient at the ground line is 0.0537 where as the corresponding analytical solution is 0.0535. Thus, the correctness of the program is verified.

5 Validation of the model with the field data

To validate the present model, the predicted values are compared with the field observations of Niigata Family Courthouse (NFCH) Building in Niigata reported by O'Rourke et al. (1994). It is reported that the NFCH building was a three-story reinforced concrete structure founded on reinforced concrete piles. During site preparation for new construction, a 350 mm diameter pile was excavated carefully and examined. Figure 2 shows the profile of the damaged pile and uncorrected standard penetration test (SPT) N values plotted with respect to depth. In the upper 7–8 m of the soil profile, the SPT values are less than 10, indicating a loose liquefiable deposit. The water table, which is considered as the upper

Fig. 2 Observed pile deformation and soil condition at NFCH building (O'Rourke et al. 1994)



boundary of the liquefiable layer, was reported to be 1.5–2.0 m below the ground surface. The pile ended in the loose sand layer. The pile showed damage at a depth of about 2.0 m from the pile top, which is the interface between the liquefiable and non-liquefiable layer. As a result of the lateral spread during the 1964 Niigata earthquake (Magnitude 7.5 and epicenter 50 km away from Niigata) the building displaced horizontally approximately 0.5–1.5 m, according to photogrammetric studies performed by Yoshida and Hamada (1991).

Predictions are made in the present study assuming N value is ≤ 10 along the length of the pile and using Eqs. (2) and (3), modulus of subgrade reaction for non-liquefied soils (k_{hn}) and modulus of deformation (E_0) of soil are evaluated. The stiffness degradation parameter (S_f) is assumed as 0.01 to take into consideration of degradation of soil stiffness due to liquefaction. The maximum soil displacement at the ground surface (g_{max}) is taken as 0.66 m, which is equal to the measured offset in the pile (O'Rourke et al. 1994).

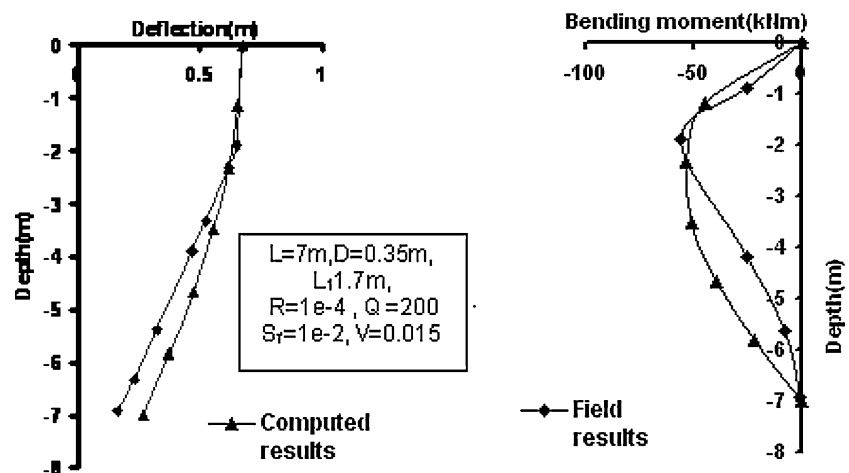
In Fig. 3, the present analytical values are compared with the observed displacements and bending moments along the length of the pile as reported by O'Rourke et al. (1994) and it is found that the maximum deflection of 672.4 mm at the pile head and the maximum deflection reported in the field is 67 m, the values being almost identical. The maximum bending moment obtained from

the present analysis is 53.8 kN m and the same observed in the field was 55.96 kN m, the error being only 4% on the conservative side. It shows a good correlation exists between the predicted results and the observed measurements. Comparison of the deflection and bending moment along the length of the pile also shows that the analysis is giving conservative results in general and thus sufficient evidence for the general acceptability of the proposed predictive model is established. It can be seen that at greater depths even though the predicted deflections are on the conservative side in comparison to the field measurements, the predicted values of bending moment shows the reverse trend; however, as the pile will be designed based on the maximum bending moment this discrepancy does not affect the predictions with regard to the safety of the design.

6 Results and discussion

Parametric study has been made and presented to bring out the influence of various parameters such as, non-liquefied depth factor ($r = L_1/L$), liquefied depth factor ($s = L_2/L$), embedded depth factor ($t = L_3/L$), pile flexibility factor ($R = EI_0/E_sL^4$), Ratio of the Young's modulus of pile and non-liquefied soil ($k = E_p/E_s$), the pile length to pile diameter ratio, i.e., the slenderness ratio ($\lambda = L/d$), soil modulus to soil strength ratio ($Q = E_s/S_u$), vertical load factor

Fig. 3 Comparison of the pile behavior obtained from the present analysis and the observations for the pile at the NFCH building (O'Rourke et al. 1994)



($V = 4P/\pi D^2 E_s$), horizontal load factor ($H = H_T/S_u D^2$), moment factor ($M = M_T/S_u D^3$), scale factor for liquefied soil (S_f), and gradient of the surface topography (sl) on the flexural behavior of pile. Analysis has been done using the following range of parameters unless otherwise specified.

$R = 0.0001, K = 500, \lambda = 25, Q = 200, V = 0-9, H = 0-25, M = 0-120, S_f = 0.01, \beta = 0.35, L_x = 0, N \leq 10$ (for liquefied soil) and ≥ 60 (for non-liquefied soil) and $sl = 1\%$.

6.1 Effect of vertical load factor

Figures 4–7 demonstrates the effect of vertical load factor, V on the flexural behavior of the pile with Free–Free end conditions. It is seen from Fig. 4 that the non-dimensional deflection at the pile head increases with the increase in V and when V exceeds a critical range of vertical load factor, it starts decreasing with the increase in V . But the non-dimensional deflection at the top interface between non-liquefied layer and the liquefied layer increases with increase in V and beyond the critical range, pile deflection at the interface becomes the maximum. The particular value of V beyond which the maximum deflection increases enormously can be termed as Critical load factor, which, in the present analysis is found to be 7.

The non-dimensional bending moment is maximum at the bottom interface between liquefied layer and the firm base (i.e., at $Z = 0.8$), which is a positive value. The maximum non-dimensional negative moment, which is usually lesser than that of the maximum non-dimensional positive bend-

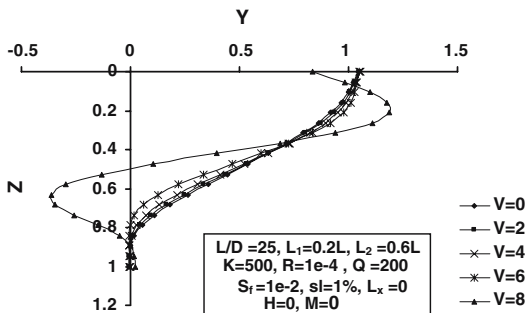


Fig. 4 Effect of V on the deflection of a Free–Free pile

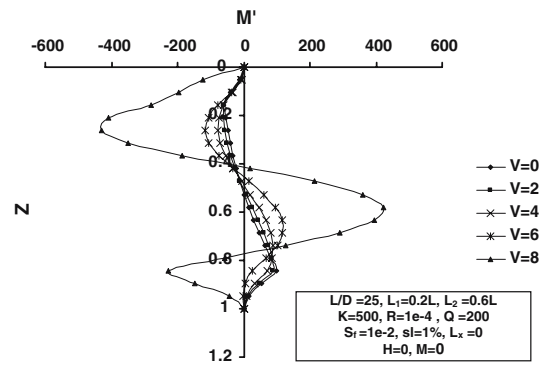


Fig. 5 Effect of V on the bending moment of a Free–Free pile

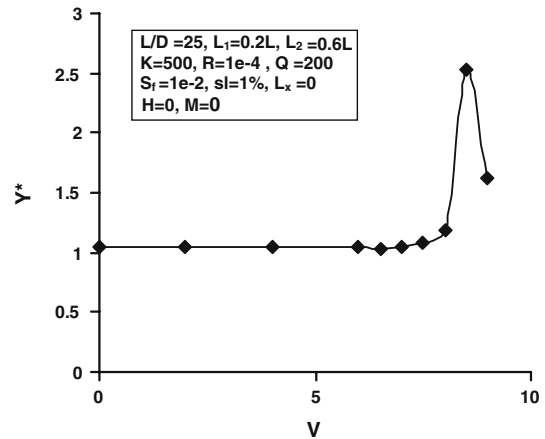


Fig. 6 Effect of V on the Y^* of a Free–Free pile

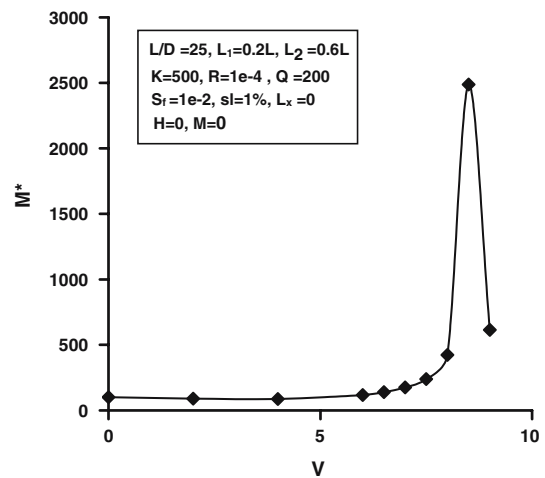


Fig. 7 Effect of V on the M^* of a Free–Free pile

ing moment, occurs at the top interface between non-liquefied layer and the liquefied layer (i.e., at $Z = 0.2$). As V increases non-dimensional bending moment also increases. Beyond the critical value of V the pile shows an abnormal increase in the bending moment (Fig. 5).

The maximum deflection coefficient and the maximum positive bending moment coefficient are referred as Y^* and M^* , respectively. Y^* shows a non-linear increase with the increase in V (Fig. 6). For $V = 0$ to $V = 7$, $Y^* = 1.04$. But beyond that Y^* shows a sharp increase to 2.5 at $V = 8.5$ and then for $V = 9$ it decreases to 1.6. M^* decreases non-linearly with increase in V (Fig. 7) and beyond $V = 4$ it increases gradually till $V = 8$ beyond which the rate of increase in its value is very high; when $V = 8.5$, the value of M^* is around 2500 and then it decreases. Generally the piles may not be designed for such a high value of bending moment and is likely to fail for the given liquefied depth and other soil data when V is equal to 8.5. For such conditions it may be more appropriate to take into account the inelastic/plastic behavior of the pile-soil interaction. From the study it has been observed that till $V = 8.5$, the developed methodology at least predicted values showing an expected trend of behavior, i.e., increased deflection with increased values of the vertical load. However, it is seen from the obtained data that for $V = 9$ the trend of behavior is different (maximum deflection decreases with the increase in V from 8.5 to 9) in contrast to the earlier one as discussed. Thus, the analysis is not reliable when the value of V exceeds 8.5.

This behavior can be explained as follows. Failure of the pile can be expected when the vertical load factor reaches the critical load factor. Also, the pile can fail before attaining the critical stage if the moment developed is greater than the yield moment of the section which can be obtained from the structural properties of the pile. This indicates that if the vertical load factor exceeds a certain value, the pile failure will occur not only because of the lateral spreading but also due to the axial load. Hence while designing the piles, care should be given not only to the lateral loads developed during the liquefaction, but also to the axial load transferred by the super structure.

6.2 Effect of depth of liquefaction

The non-liquefied depth factor, r is varied from 0 to 0.8. The embedded depth is taken to be constant throughout the analysis as 20% of the length of the pile. When there is no liquefaction, i.e., when $r = 0.8$, the pile shows zero values of Y and M' , which validates the correctness of the developed program (Figs. 8 and 9). As the non-liquefied depth factor decreases to zero, i.e., when the liquefaction is starting from the ground surface itself, the Y at the pile top increases to its maximum value, which is around $1.2D$ compared to zero when there was no soil liquefaction at all. But the Y in liquefied region is more when the non-liquefied depth is larger. This is because the relative displacement of the pile and the soil is more when the non-liquefied depth is larger and

Fig. 8 Effect of r on the deflection

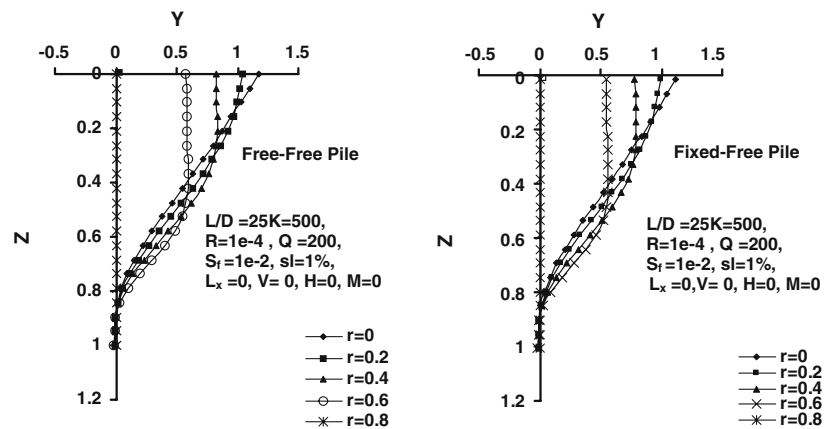
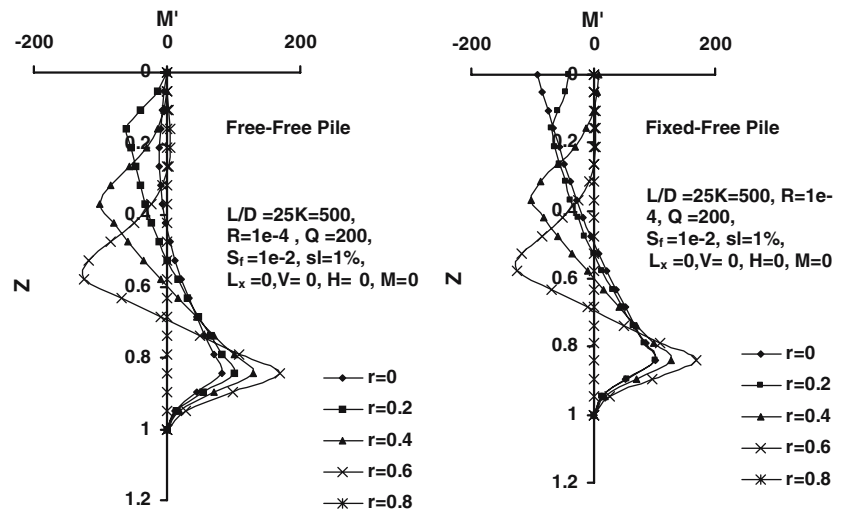


Fig. 9 Effect of r on the bending moment



this results in the increase of lateral soil pressure. It will lead to the increase of deflection in the liquefied zone and also an increase in the values of M^* from 82 to 168, which occurs at $Z = 0.8$ (Fig. 10). Thus M^* increases with r and suddenly drops to zero when $r = 0.8$. For both the end conditions Y^* decreases and M^* increases with increase in r . Only in the range $r = 0$ to $r = 0.2$,

the end condition will influence the flexural behavior of pile. In this range Free-Free pile will have more Y^* than that of Fixed-Free pile and reverse is the case for M^* .

Under lateral loading, when r is increased from 0 to 0.4, the Y^* decreases by 30% for all the combinations of H and M . The figures show similar trend of behavior when the values of r are

Fig. 10 Effect of r on Y^* and M^*

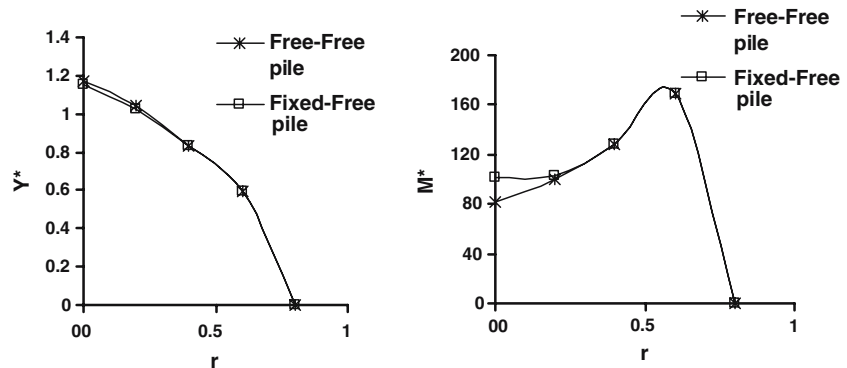


Fig. 11 Effect of r on Y^* of Free-Free pile under lateral loading

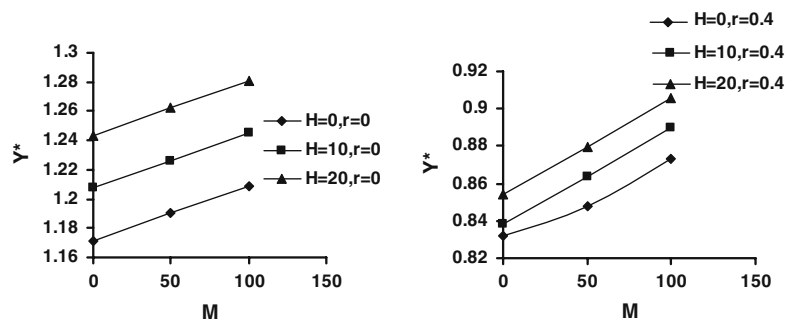
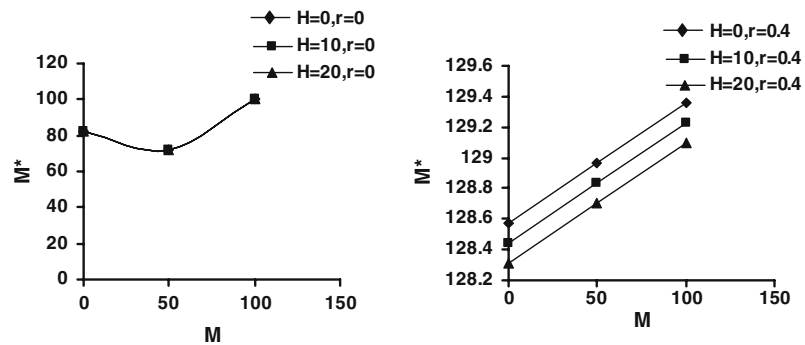


Fig. 12 Effect of r on M^* of Free-Free pile under lateral loading



0 and 0.4, respectively. The M^* initially decreases and then increases with the applied moment factor at $r = 0$. But, in contrast when $r = 0.4$, M^* all the time increases with increase in the lateral loads. The lateral soil pressure contributes to the increase in M^* . The results are shown in Figs. 11 and 12.

7 Conclusions

Based on the studies conducted above the following conclusions can be drawn:

- (i) The developed generalized procedure for the analysis of flexural behavior of axially and laterally loaded piles under liquefied soil condition assuming the validity of the concept of modulus of subgrade reaction quantifying the forces exerted by the spreading liquefied soil as proposed by Tokimatsu (1999) has been found to be reliable.
- (ii) The response of the piles as found by using the proposed model are found to be in excellent agreement with theoretical and experimental values reported in literature.
- (iii) The axial load has a significant importance on the response of pile foundations in lateral spreading areas. A pile which is otherwise safe under normal conditions may fail when it loses support from the surrounding soils due to either partial or full soil liquefaction. In addition to the loss of support, the piles may experience large drag force due to the moving soil especially for riverfront structures.
- (iv) As the vertical load factor reaches a critical value, the pile may fail due to buckling. The developed bending moment will be very high at critical loading and it may exceed the yield moment of the section and hence the failure can take place. Therefore, the current method of pile design based on bending mechanism is not appropriate and, for the safe design consideration of axial loads also is very important.
- (v) The depth of top non-liquefied layer plays an important role in the flexural behavior of piles in liquefiable areas. The densification of the soil in the liquefiable areas and a proper top non-liquefied soil cover will cause an appreciable reduction in the destruction.
- (vi) The developed computer program can be used effectively to predict the deflection and bending moment of the piles under various conditions of loading, soil profile, and pile characteristics.

References

- Abdoun T, Dobry R (2002) Evaluation of pile foundation response to lateral spreading. *Soil Dyn Earthquake Eng* 22:1051–1058
- Barlett SF, Youd TL (1995) Empirical prediction of liquefaction induced lateral spread. *J Geotec Eng ASCE* 121(4):316–329
- Basudhar PK, Mishra SK, Maheshwari P, Das SK (2002) Flexural analysis of laterally loaded piles under liquefied soil conditions, *Proceedings Indian Geotechnical Conference, Geotechnical Engineering: Environmental Challenges*. Allahabad, India, 435–440
- Berrill JB, Christensen SA, Keenan RP, Okadas W, Pettinga JR (2001) Case study of lateral spreading

- forces on a piled foundation. *Geotechnique* 51(6):501–517
- Bhattacharya S (2004) A method to evaluate the safety of the existing piled foundations against buckling in liquefiable soils. In: First international conference on urban earthquake engineering, Tokyo, Japan, 339–346
- Hamada M, O'Rourke YD (1992) Case studies of liquefaction and lifeline performance during fast earthquakes, Technical report, NCEER-92-0001
- Hamada M, Yasuda S, Isoyama R, Emoto K (1986) Study on liquefaction-induced permanent ground displacements, Association for the development of earthquake prediction, Tokyo, Japan
- Hetenyi M (1946) Beams on elastic foundations. University of Michigan Press, Ann Arbor, Mich
- Ishihara K (1997) Geotechnical aspects of the 1995 Kobe earthquake. In: Proceedings of the 14th international conference on soil mechanics and foundation engineering. Terzaghi Oration, Hamburg, 2047–2073
- Ishihara K, Cubrinovski M (1998) Soil–pile interaction in liquefied deposits undergoing lateral spreading. In: Maric B et al (eds) Geotechnical hazards. Balkema, 51–64
- Klar A, Baker R, Frydman S (2004) Seismic soil–pile interaction in liquefiable soil. *Soil Dyn Earthquake Eng* 24:551–564
- Mishra SK (1992) Analysis of laterally loaded piles under liquefied soil conditions. M. Tech thesis, Indian Institute of Technology, Kanpur
- Miyajima M, Kitaura M (1994) Experiments on force acting on underground structures in liquefaction-induced ground flow, Technical Report NCEER-94-0026, NCEER, Buffalo, NY, 445–455
- O'Rourke TD, Meyersohn WD, Shiba Y, Chaudhuri D (1994) Evaluation of pile response to liquefaction-induced lateral spread, Technical Report NCEER-94-0026, NCEER, Buffalo, NY, 457–479
- Shamoto Y, Zhang JM, Tokimatsu K (1998) Methods for predicting residual post-liquefaction ground settlement and lateral spreading. *Soils Found* 38(special issue):69–83
- Tamri Y, Towhata I (2003) Seismic soil-structure interaction of cross sections of flexible underground structures subjected to soil liquefaction. *Soils Found* 43(2):69–87
- Tokimatsu K, Oh-oka H, Satake K, Shamoto Y, Asaka Y (1998) Effects of lateral ground movements on failure patterns of piles in the 1995 Hyogoken-Nambu earthquake, ASCE, Geotechnical earthquake Engrg and soil dynamics 3rd Conf., 1175–1186
- Tokimatsu K (1999) Performance of pile foundations in laterally spreading soils, Proc 2nd international conf. on Earthquake Geotechnical Engineering, Lisbon, Portugal, 957–964
- Yoshida N, Hamada M (1991) Damage to foundation piles and deformation pattern of ground due to liquefaction-induced permanent ground deformations, 3rd US–Japan workshop on earthquake-resistant design of lifeline facilities and countermeasures for soil liquefaction, Technical report NCEER-91-0001, NCEER, Buffalo, NY, 147–161
- Zhang G, Robertson PK, Brachman RWI (2004) Estimating liquefaction induced lateral displacements using the standard penetration test or cone penetration test. *J Geotec Geoenviron Eng* 130(8):861–871